

NEGF-DFT Study on Tuning Electrical Conductivity of Benzene-1, 4-dithiol

AHMED M. EL-NAHAS^{1*}, EL-SAYED R. KHATTAB¹,
MORAD M. EL-HENDAWY² and AHMED H. MANGOOD¹

¹Department of Chemistry, Faculty of Science, El-Menoufia University,
Shebin El-Kom, Egypt

²Department of Chemistry, Faculty of Science, Assuit University,
New Valley Campus, Egypt

amelnahs@hotmail.com

Received 17 December 2015 / Accepted 11 January 2016

Abstract: In this paper, tuning electrical conductivity of benzene-1,4-dithiol (**M0**) has been done through sequential substitute of the CH groups by nitrogen atoms in the molecular skeleton of the benzene ring and constitutional isomery. *I-V* characteristics of seven derivatives of **M0** using non-equilibrium Green's function (NEGF) approach combined with density functional theory (DFT) have been investigated. Our findings have been interpreted in terms of transmission spectra and molecular projected self-consistent Hamiltonian (MPSH). The results obtained show a slight effect on the conductivity at low bias with the insertion of nitrogen atoms in the benzene ring while an increase in the conductivity is observed at high bias. The results also showed that constitutional isomery significantly affects the *I-V* behavior of the diazabenzenes at all applied voltages, at a given bias the current varies by 30-40%. The data give the following conductivity order: pyrimidine-1,4-dithiolate > pyrazine-1,4-dithiolate > pyridazine-1,4-dithiolate. These findings indicate that the structural factors would be helpful for designing molecular wires for nanoscale applications.

Keywords: Benzene-1,4-dithiol, Molecular wire, NEGF-DFT, Transmission spectra, Isomery effect

Introduction

Benzene-1,4-dithiol (**M0**) is considered as a good example to investigate electron transport and functionality of molecular junctions in the field of organic electronics. Both experiment¹⁻⁴ and theory⁵⁻²⁰ have been interested in reporting and understanding electron transport properties of **M0** and its derivatives. For instance, Reed *et al.*,¹ measured the *I-V* characteristics of **M0** using the mechanically controllable break junction. The results illustrated a conductance voltage curve of two steps in both bias directions. Using the same technique, Teramae *et al.*,² plotted the *I-V* curve of Au/ **M0** /Au junction and found a break down voltage with a broad distribution and takes a maximum at about 1.2-1.5 volt. Also, Horiguchi *et al.*,⁴ recorded the conductance of Ni/ **M0** /Ni junctions under static magnetic

fields up to 250 mT at cryogenic temperatures and statistically demonstrated the magnetic-field dependence of the single-molecule conductance. They reported increasing of the single-molecule resistance with field strength until it reaches its maximum limit at 50 mT leading to magnetic resistance of 80% -90% at 77 K.

The non-equilibrium Green functions combined with the density functional theory (NEGF-DFT)⁵⁻²⁰ reported electron transport through **M0** with regard to its structures and derivatives, nature of electrode and anchors. Seminario *et al.*,⁵ studied the effect of electrode nature on conductance of **M0**. They carried a comparative study between thio and isonitrile groups as anchors with metals of groups 10 (Ni, Pd and Pt) and 11 (Cu, Ag and Au). The data predicted that the best metal for the metal-molecule interface is Pd. As for the structure of **M0**, it has two conformations and excitation of the molecule causes it to change from one form to another and switch between a strongly and a weakly conducting state⁷. The face conformation recorded high conductivity 'ON' while *edge* structure displayed weak conduction 'OFF'.

Tuning electrical conductivity of a given molecule could be achieved through a various means such as constitutional isomery¹⁰, oligomerization¹¹⁻¹³ and anchors^{5,14-17}. Cheng *et al.*,¹⁰ studied the isomery effect on the electron transport through **M0**. They studied three isomers of diazabenzene, namely pyrimidine, pyrazine and pyridazine and concluded that the relative positions of the two nitrogen atoms can significantly affect the transport behavior due to change of the electronic structure of the molecule. The current project used NEGF-DFT approach to highlight how chemistry can change the electrical conductivity via two molecular structural factors: sequential substitute of the CH groups by nitrogen atoms in the skeleton of benzene ring and the constitutional isomery. Figure 1 displays chemical structures of the investigated molecules which are classified into two groups: **A** and **B**. *I-V* curves, transmission spectra, energy levels and spatial distributions of frontier molecular orbitals were analyzed.

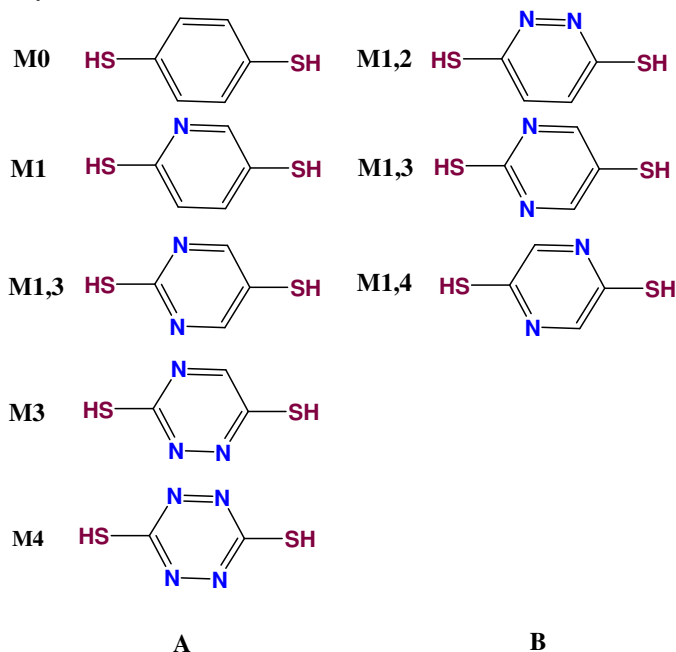


Figure 1. Chemical structures of studied molecules

Computational methodology

All isolated molecules were optimized using B3LYP/6-31G(d,p)²⁵⁻²⁷ as implemented in Gaussian 09 package²⁸. Based on the optimized structures, the *I-V* characteristics were computed through two-probe system as a function of applied bias using the combined DFT and non-equilibrium Green's function (NEGF) formalism as implemented in Atomistic ToolKit code (ATK 2008.10)²⁹⁻³². The two-probe systems were built by wiring the selected molecule (–S–M–S–) between two gold electrodes as depicted in Figure 2. The hydrogen atoms of anchoring thiol groups were removed when the molecules come in contact with the electrodes. Each molecule was forced to be perpendicular to the gold surface by placing sulfur atoms above the three fold hollow site with initial distance of 2.3 Å above the gold surface, which is in the reasonable range of 1.90-2.39 Å as used by most authors. The scattering region consists of the wired molecule as well as part of the left and right electrodes where the screening effect takes place. Each layer in the gold electrode is represented by (3x3) supercell with the periodic boundary conditions. The exchange correlation function is described by local density approximation (LDA)³³. Double zeta with polarization (DZP) basis set was used for all atoms except gold atoms where single zeta with polarization (SZP) function was assigned. The voltage is steadily increased from 0.0 to 4 V. The steady state current through a two-probe system is computed from the Landauer-Buttiker formula³⁴.

$$I = \frac{2e}{h} \int_{\mu_R}^{\mu_L} T(E, V) dE$$

Where $T(E, V)$ is the transmission coefficient for electrons with energy E at bias V ; μ_L and μ_R are the electrochemical potential of the left and right electrodes, respectively. The energy region which contributes to current integral is called bias window³⁵. It is given by $\mu_L = E_F - eV_b/2$ and $\mu_R = E_F + eV_b/2$, E_F is the average Fermi energy level and set as zero.

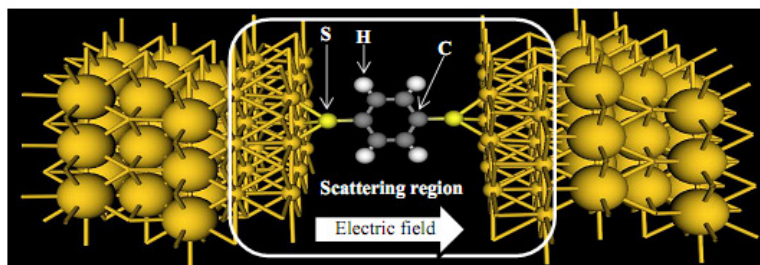


Figure 2. Sketch of a representative two-probe system used to compute *I-V* curve. The tested junction (here **M0**) is sandwiched between (3x3) two gold surfaces Au (111). Region within the frame is the scattering region.

Results and Discussion

Insertion of nitrogen atom(s)

I-V characteristics

The *I-V* curves of five molecules (**M0**, **M1**, **M1,3**, **M3** and **M4**) designated as group **A** (Figure 1) are displayed in Figure 3 where one, two, three or four nitrogen atoms have been inserted into skeletal of the benzene ring. The *I-V* behavior of **M0** and **M1** over the whole range of the applied voltage is almost similar. Below 2 V, the current through the five molecules are comparable indicating a slight effect of the inserted nitrogen atoms in this bias range. The current pass through all of the investigated molecules exhibits an Ohmic

character below 1.5V. Above this volt, a break in the I - V characteristics was observed. At 4 V, the current produced from **M3** and **M4** (100, 120 μ A, respectively) is higher than **M0** of 81.2 μ A by 23% and 47%. It is worth mentioning that the current pass through **M4** is much higher than that of the remaining molecules. To understand some details about the properties of electron transport through these systems, the transmission spectra of the investigated junctions were analyzed in the next section.

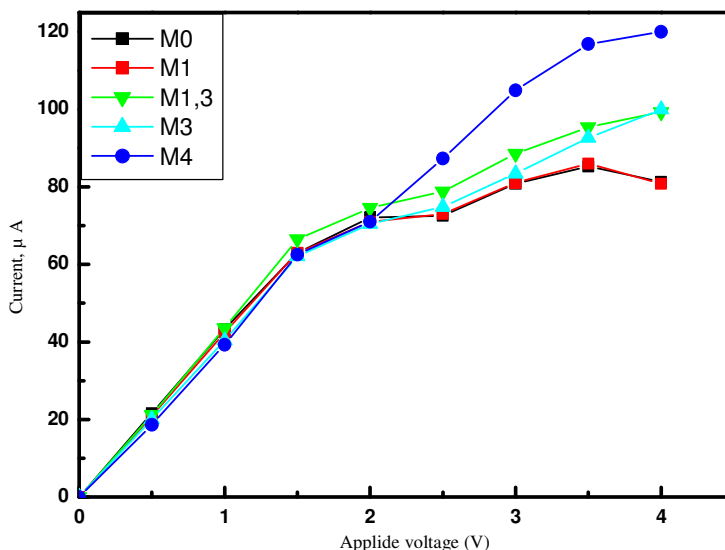


Figure 3. I-V curve for group A molecules

Transmission spectra analysis

Figure 4 depicts the transmission spectra of group A molecular junctions under the applied biases of 0-4 V. Bias window is given as a filled region in Figure 4. The transport properties of the **M0**-based molecules can be explained in term of spatial distribution of the frontier molecular orbitals around the Fermi level, namely highest occupied molecular orbital (HOMO) and lowest unoccupied molecular orbital (LUMO). The first peak below and above the Fermi energy can be related to resonance of HOMO and LUMO, respectively. Under zero bias, the main feature of transmission spectrum of **M0** is the existence of a broad resonance peak just below the Fermi level (HOMO peak) and a narrower peak at ~ 3 eV (LUMO peak), which agrees with Stokbro *et al.*, findings¹⁵. Upon increasing bias, the HOMO peak broadens and its shoulder appears in the bias window. At a bias of 3 V, the HOMO peak and the shoulder of the second transmission peak (HOMO-1) get into the bias window. HOMO and HOMO-1 peaks at 4 V are completely shifted to the bias window. This might explain the increase in the current with rising of bias as demonstrated in Figure 3. **M1** shows the same feature of **M0**.

The transmission spectra of **M1,3** and **M3** are similar under the whole range of applied voltages. Below 2 V, no peaks could be found in the bias window. However, above this bias voltage, the shoulder of the first transmission peak enters the bias window gradually until 4 V where both the first and second transmission resonance peaks move to the bias window. Their transmission coefficients are larger than those of **M0** and **M1** as depicted in Figure 5.

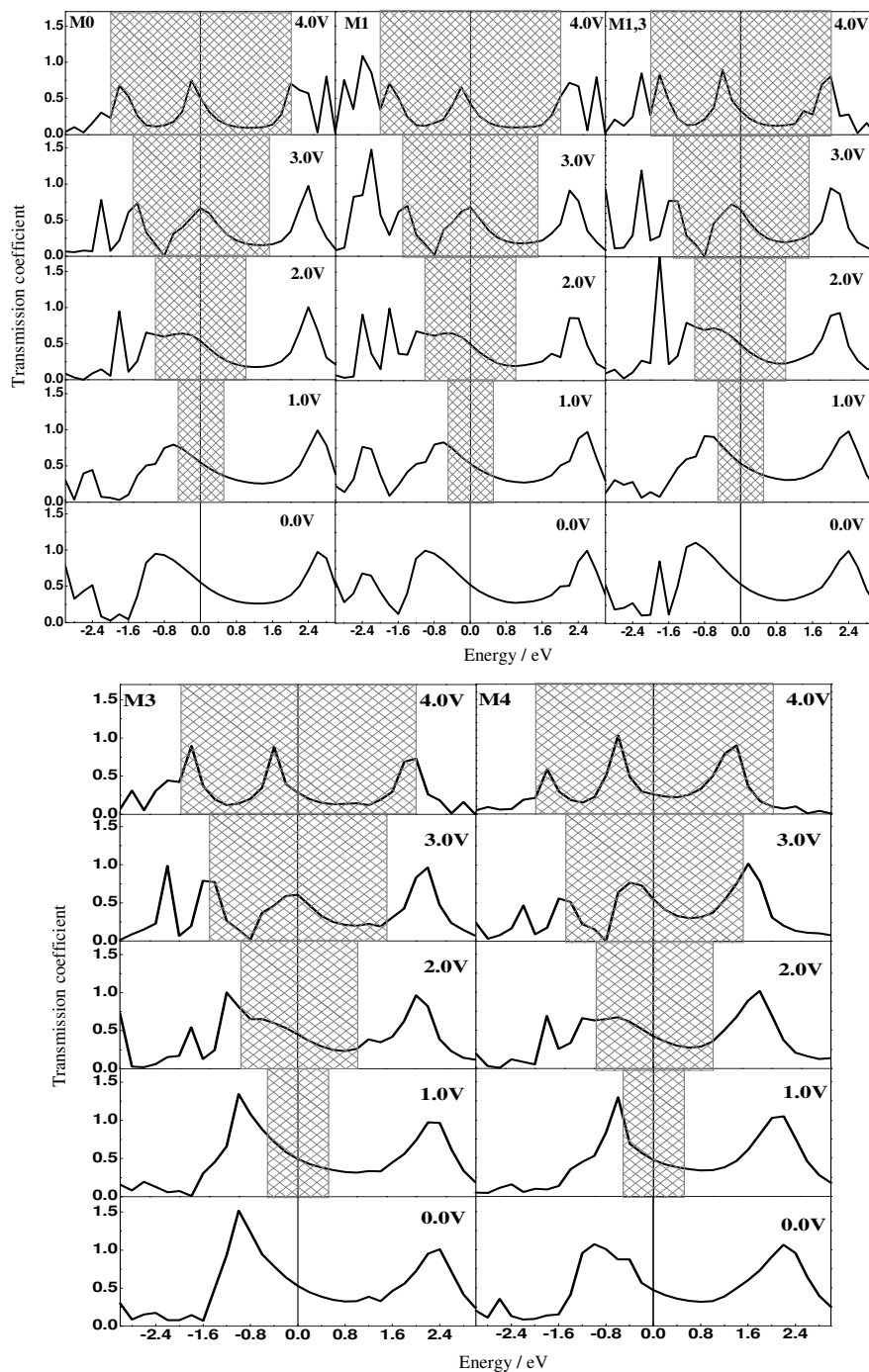


Figure 4. Transmission spectra of M0, M1, M1,3, M3 and M4 molecular wires under different applied bias. The filled region is the bias window

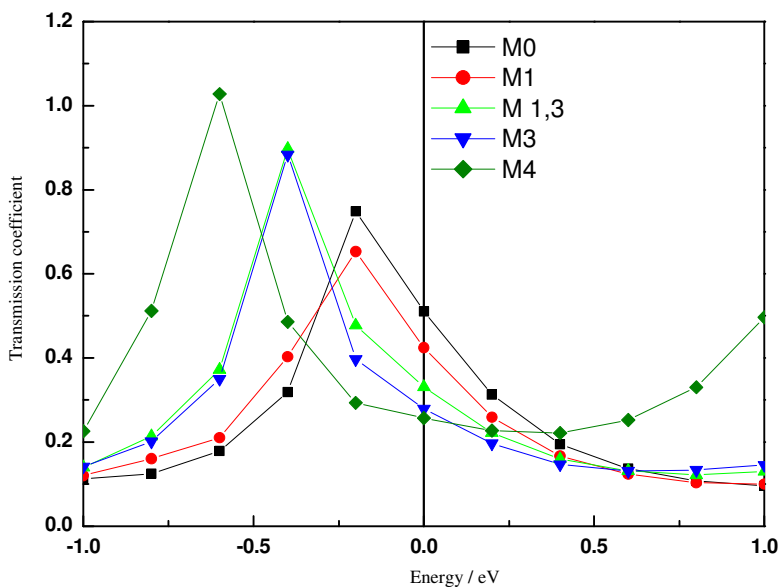


Figure 5. Transmission spectra of group **A** molecules at 4V

For **M4**, the first resonance peak above the Fermi energy is highly sensitive to the applied voltage. Upon increasing bias it was shifted toward the Fermi level until it completely gets into the bias window at 4 V. Also, the first and second transmission peaks of **M4** below the Fermi level totally enter the bias window at 4V. Therefore, **M4** has three transmission peaks in the bias window leading to the observed remarkable increase in the current as shown in Figure 3.

The height of the transmission peaks in the bias windows reflects the extent of molecular conductance *i.e.* better molecular conductor is obtained from peaks with higher transmission coefficients in the bias window. It is noticed from Figure 5 that the transmission coefficient of the main resonance peak is significantly affected by the number of the nitrogen atoms. For instance, the transmission coefficients of the main peak for **M1,3** and **M3** are much larger than those of **M0** and **M1**. This correlates with the current-voltage curve. For example, **M4** is the best conductor among the studied molecular junctions as it has the largest transmission coefficient of the main resonance peak³⁶.

MPSH Eigenstates analysis

The transmission spectra of the investigated molecular junctions under different bias voltages can be interpreted in terms of frontier molecular orbitals around the Fermi energy level. This can be done by calculating molecular projected self-consistent Hamiltonian (MPSH). The MPSH Eigenstates reflect the energy levels of the molecule in the presence of the electrodes. The spatial distributions of these orbitals are displayed in Figure 6. In general, MPSH orbitals which are fully delocalized over the molecular backbone will give peaks in the relevant transmission spectra³⁶⁻³⁸ and states which are localized on one side, on the center of molecule, or on the two electrodes will not give any peaks. The spatial distribution of frontier orbitals on the anchors is an important parameter for high electrical conductivity. For **M0**, the first and the second transmission peaks below the Fermi level can be related to HOMO and HOMO-3, respectively. For **M1**, the first and second transmission peaks below the Fermi energy can be related to HOMO and HOMO-1, respectively.

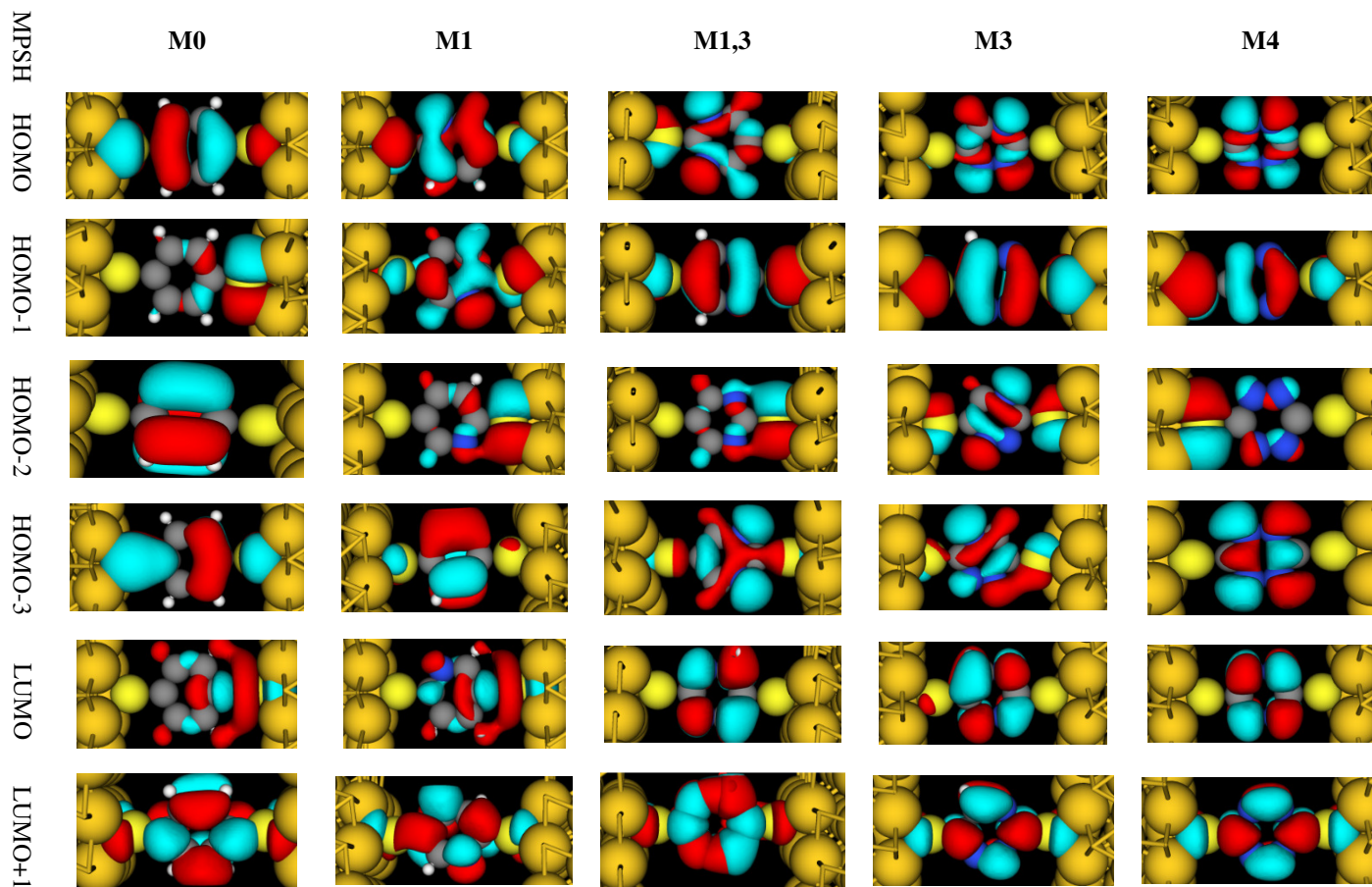


Figure 6. Spatial distribution of MPSH HOMO, HOMO-1, HOMO-2, HOMO-3 LUMO, and LUMO+1 for M0, M1, M1,3, M3 and M4 at 4V and the isovalue of molecular orbitals is 0.05 e au^{-3}

For **M1,3** the first and second transmission peaks below the Fermi energy reflect HOMO-1 and HOMO-3. The first and second peaks below the Fermi level produced from **M3** and **M4** can be related to the resonance of HOMO-1 and HOMO-2, respectively. For all molecular systems, the first transmission peak above the Fermi energy can be attributed to the resonance of LUMO+1. Also we can interpret the higher conductivity of some junctions like **M1,3**, **M3** and **M4** in the light of theory presented by Ernzerhof and Rocheleau³⁹, where they proposed that increasing the orbital density on the anchors increases charge transport through molecular device. For **M1,3** and **M3**, the HOMO-1 orbital is fully delocalized over the molecular backbone with high orbital density on the anchors. In this respect, **M4** seems the best conductor where its HOMO-1 orbital is fully delocalized with orbital density on clips atoms higher than other molecules.

Eigenvalues of MPSH

Figure 7 illustrates the eigenvalues of HOMO and LUMO for group A molecules under zero bias. An inspection of this figure indicates that LUMO energy decreases with increasing number of nitrogen atoms (from 2.18 eV for **M0** to 0.89 eV for **M4**), while HOMO energy shows the opposite trend (from -1.97 eV for **M0** to -0.36 eV for **M4**). Therefore, the HOMO-LUMO gap (HLG) is significantly decreased by increasing number of nitrogen atoms (from 4.15 eV for **M0** to 1.25 eV for **M4**), which matches the *I-V* behavior of these molecules. Moreover, the eigenvalues of HOMOs are much closer to the Fermi level than LUMOs for all molecules which means that the current pass through these systems is driven by electron rather than hole transport^{35,38}.

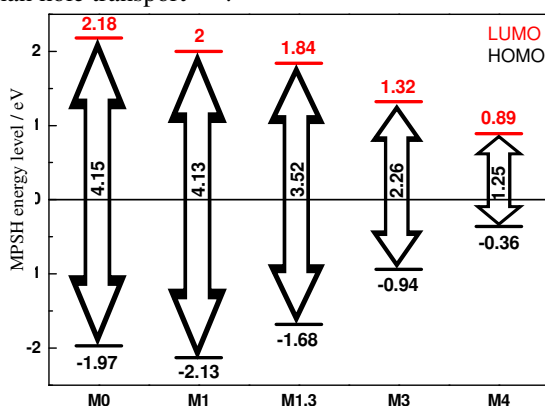


Figure 7. The HOMO and LUMO energy levels of group A molecules at zero bias. Fermi level of the electrode is set to zero

Isomery effect

Previously, we studied the effect of insertion of nitrogen atom(s) in the junction backbone on the rectifying property of diblock molecular diode⁴⁰. A regular change in the electronic structure and electrical property was observed in a wide range of applied electric field.

I-V characteristics

The *I-V* characteristics of three molecular devices of isomers with two nitrogen atoms at different positions in the benzene ring were investigated. These isomers are designated as **M1,2**, **M1,3** and **M1,4** for the nitrogen atoms occupying ortho, meta and para positions, respectively, as given in Figure 1. Obviously, the constitutional isomerism significantly affects the *I-V* behaviour of the three devices along the whole rang of applied bias voltages,

(Figure 8). For instance, under the effect of 2.5 volt the electric current pass through **M1,2**, **M1,3** and **M1,4** was 50.6, 78.8 and 68.3 μA , respectively, which indicates higher conductivity of **M1,3** relative to **M1,4** and **M1,2**.

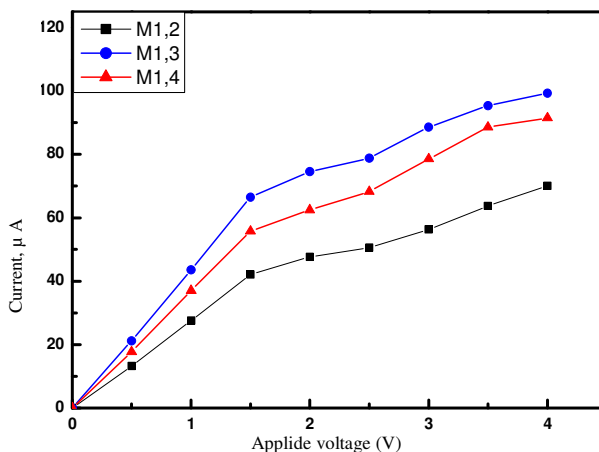


Figure 8. *I-V* behavior of group **B** molecules

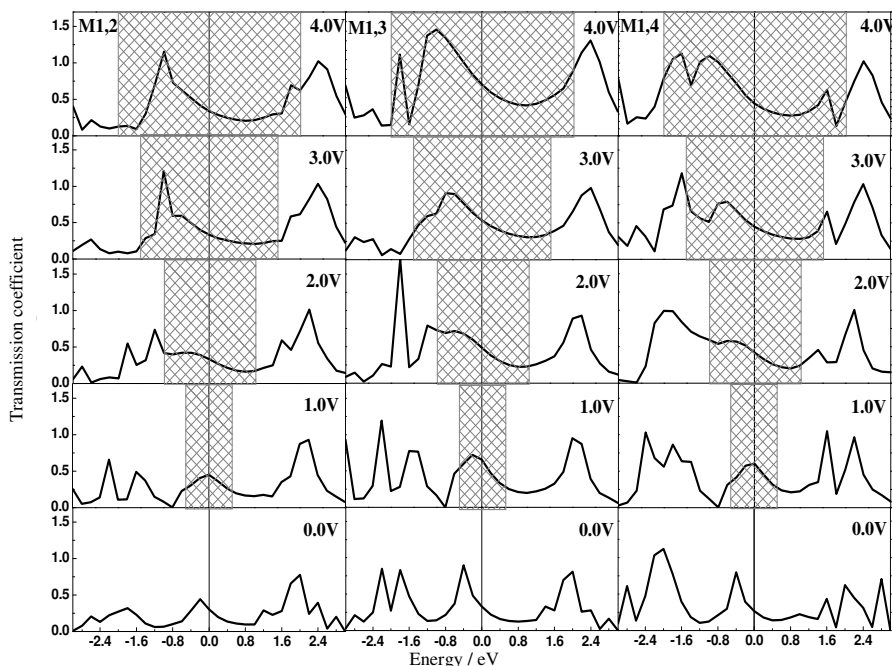


Figure 9. Transmission spectra of **M1,2**, **M1,3** and **M1,4** molecular wires under different applied bias. The filled region is bias window

Transmission spectra

Figure 9 shows the transmission spectra of group **B** junctions. In the case of **M1,2**, no transmission peaks were observed in the bias window below 2 V. However, at a bias of 2 V the shoulder of the first transmission peak below the Fermi energy moves to the bias window,

but the transmission coefficient is very small which implies limited current as illustrated in Figure 6. At 4 V, the whole first transmission peak (main peak), the shoulder of the second peak below the Fermi level and the first transmission peak above the Fermi energy level enter the bias window. The value of the transmission coefficient of the main peak is small compared to those of **M1,3** and **M1,4**. Consequently, the current pass through **M1,2** is smaller than that of the other two molecular systems.

For **M1,4**, the shoulder of the first transmission peak gets into the bias window at 1V with a very small transmission coefficient. With increasing the bias to 2V, the shoulder of the first transmission peak enters the bias window with the transmission coefficient of the main peak being larger than that of **M1,2**. At a bias voltage of 4V, the first transmission peak below the Fermi level and the first peak above the Fermi level completely move to the bias window region. The transmission coefficient of the higher energy peak in the bias window is very small, so it doesn't affect current significantly.

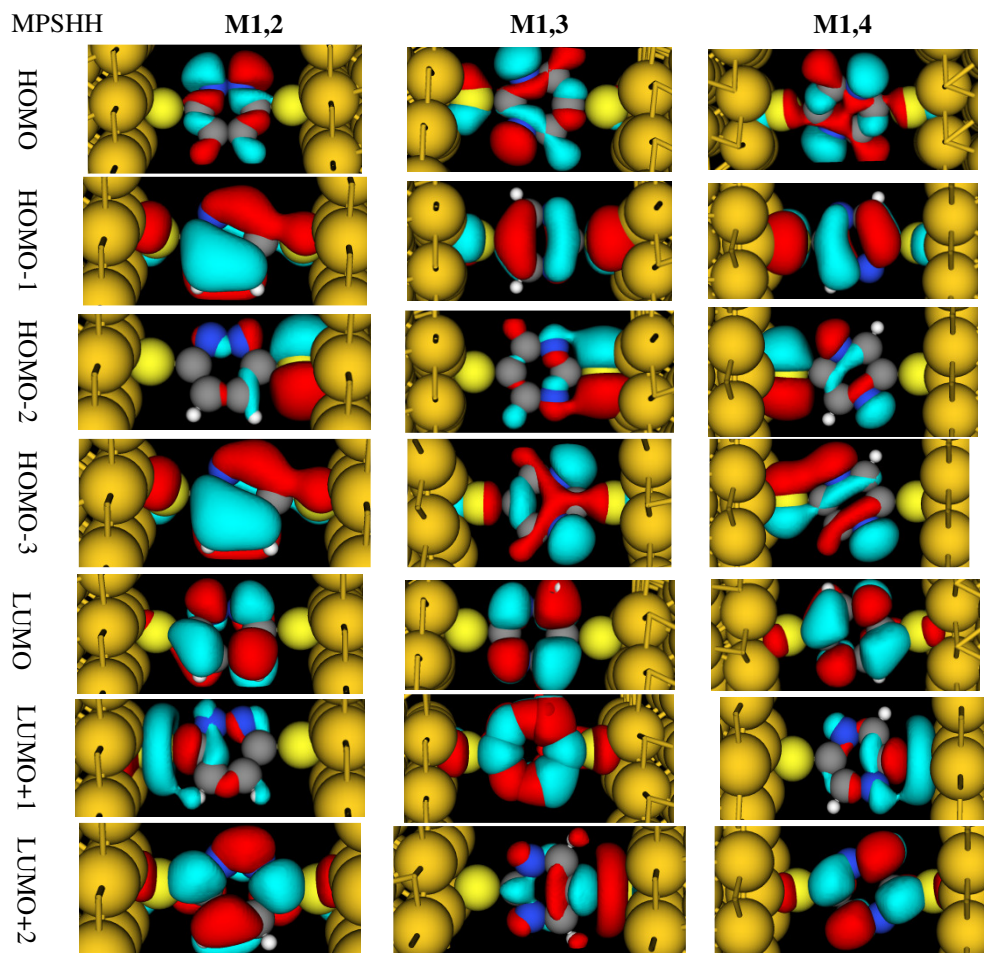


Figure 10. Spatial distribution of MPSH HOMO, HOMO-1, HOMO-2 HOMO-3 LUMO, LUMO+1 and LUMO+2 for **M1,2**, **M1,3** and **M1,4** at 4V and the isovalue of molecular orbitals is 0.05 e au^{-3}

At 1V, the transmission coefficient of the main peak of **M1,3** is larger than that of **M1,4**. The entire first transmission peak and half of its next peak below the Fermi energy enter the bias window at 3V. However, with increasing bias to 4V, both first and second transmission peaks below the Fermi energy level are completely shifted to the bias window along with the shoulder of the first transmission peak above the Fermi level leading to a remarkable increase in the current.

MPSH Eigenstates

Figure 10 collects the MPSH Eigenstates of group **B** molecules. For **M1,2** and **M1,3**, the first and second transmission peaks below the Fermi energy can be related to the resonance of HOMO-1 and HOMO-3, respectively. However, the first peak above the Fermi level corresponds to LUMO+2 and LUMO+1 resonance for **M1,2** and **M1,3**, respectively. For **M1,4**, the first and second peaks below Fermi level reflects the resonance of HOMO and HOMO-1, respectively, while the first transmission peak above the Fermi level can be related to the resonance of LUMO. Also the orbital density on the anchors follows the order **M1,2**, **M1,4** and **M1,3**. This could explain the *I-V* behavior.

Conclusion

Density functional theory (DFT) in conjunction with non-equilibrium Green's function method (NEGF) was used to investigate the *I-V* properties of benzene-1,4-dithiol (**M0**) with systematic insertion of nitrogen atoms in the benzene ring and constitutional isomery of diazabenzene. Our findings demonstrated that the increment of number of nitrogen atoms significantly increases the current by about 47% especially at high bias voltage. The sequential substitute of nitrogen atoms shifts the main transmission peak to the bias window which leads to sharp increase in the current pass through the relevant molecular system. The MPSH Eigenstates indicated that the increment of nitrogen atoms increases orbital density on the anchors which strengthens coupling between the molecular junction and two electrodes. The results also showed that constitutional isomery significantly affects the *I-V* behavior of the diazabenzenes at all applied voltages, at a given bias the current varies by 30-40%. The results reported in this paper shed light on two structural factors that may be utilized for improvement and/or rational design of functionalized molecular devices.

Acknowledgments

Authors would like to thank the Quantum wise Company for providing the license of ATK code, especially Dr. Marcus Yee, Quantum wise A/S, www.quantumwise.com

References

1. Reed M A, Zhou C, Muller C J, Burgin T P and Tour J M, *Science*, 1997, **278**(5336), 252-254.
2. Teramae Y, Horiguchi K, Hashimoto S, Tsutsui M, Kurokawa S and Sakaia A, *Appl Phys Lett.*, 2008, **93**(8), 083121-083124; DOI:10.1063/1.2976666
3. Kim L, Kim J, Gu G H and Suh J S, *Chem Phys Lett.*, 2006, **427**(1-3), 137-141; DOI:10.1016/j.cplett.2006.03.104
4. Horiguchi K, Sagisaka T, Kurokawa S and Saka A, *J Appl Phys.*, 2013, **113**, 144313-144319.
5. Seminario J M, De La Cruz C E and Derosa P A, *J Am Chem Soc.*, 2001, **123**(23), 5616-5617; DOI:10.1021/ja015661q

6. Geng W T, Nara J and Ohno T, *Thin Solid Films*, 2004, **464-465**, 379-383; DOI:10.1016/j.tsf.2004.06.083
7. Ganji M D and Rungger I, *J Iran Chem Soc.*, 2008, **5(4)**, 566-573; DOI:10.1007/BF03246135
8. Schwingenschlogl U and Schuster C, *Chem Phys Lett.*, 2007, **435(1-3)**, 100-103; DOI:10.1016/j.cplett.2006.12.049
9. Nara J, Higai S, Morikawa Y and Ohno T, *Appl Surf Sci.*, 2004, **237**, 433-438.
10. Cheng W W, Chen H, Note R, Mizuseki H and Kawazoe Y, *Physica E*, 2005, **25(4)**, 643-646; DOI:10.1016/j.physe.2004.09.006
11. Wang L, Li S Y, Yuan J H, Gu J Y, Wang D and Wan L J, *Chem Asian J.*, 2014, **9(8)**, 2077-2082; DOI:10.1002/asia.201402196
12. Haiss W, Zalinge H, Higgins S J, Bethell D, Hçbenreich H, Schiffrin D J and Nichols R J, *J Am Chem Soc.*, 2003, **125(50)**, 15294-15295; DOI:10.1021/ja038214e
13. Kopf A and Saalfrank P, *Chem Phys Lett.*, 2004, **386(1-3)**, 17-24; DOI:10.1016/j.cplett.2003.12.118
14. Bauschlicher Jr C W, Ricca A, Mingo N and Lawson J, *Chem Phys Lett.*, 2003, **372(5-6)**, 723-727; DOI:10.1016/S0009-2614(03)00486-X
15. Stokbro K, Taylor J, Brandbyge M, Mozos J L and Ordejon P, *Comp Mater Sci.*, 2003, **27(1-2)**, 151-160; DOI:10.1016/S0927-0256(02)00439-1
16. Souza A M, Rungger I, Pontes R B, Rocha A R, Schwingenschlogl U and Sanvito S, *Nanoscale*, 2014, **6**, 14495-14507; DOI:10.1039/C4NR04081C
17. Nara J, Kino H, Kobayashi N, Tsukada M and Ohno T, *Thin Solid Films*, 2003, **438-439**, 221-224; DOI:10.1016/S0040-6090(03)00774-0
18. Bauschlicher Jr C W and Ricca A, *Chem Phys Lett.*, 2003, **367(1-2)**, 90-94; DOI:10.1016/S0009-2614(02)01626-3
19. Bauschlicher Jr C W, Lawson J W, Ricca A, Xue Y, Ratner M A, *Chem Phys Lett.*, 2004, **388(4-6)**, 427-429; DOI:10.1016/j.cplett.2004.03.038
20. Chen X C, Xu Y and Zeng Z Y, *Physica B*, 2008, **403(17)**, 2597-2601; DOI:10.1016/j.physb.2008.01.050
21. Derosa P A and Seminario J M, *J Phys Chem B*, 2001, **105(2)**, 471-481; DOI:10.1021/jp003033+
22. Piccinin S, Selloni A, Scandolo S, Car R and Scoles G, *J Chem Phys.*, 2003, **119(13)**, 6729-6735; DOI:10.1063/1.1602057
23. Damle P, Ghosh A W and Datta S, *Chem Phys.*, 2002, **281(2-3)**, 171-187; DOI:10.1016/S0301-0104(02)00496-2
24. Cacelli I, Ferretti A, Girlanda M and Macucci M, *Chem Phys.*, 2007, **333(1)**, 26-36; DOI:10.1016/j.chemphys.2006.12.021
25. Becke A D, *J Chem Phys.*, 1993, **98**, 5648-5652; DOI:10.1063/1.464913
26. Lee C, Yang W and Parr R G, *Phys Rev B*, 1988, **37(2)**, 785-789; DOI:10.1103/PhysRevB.37.785
27. Stephens P J, Devlin F J, Chabalowski C F and Frisch M J, *J Phys Chem.*, 1994, **98**, 11623-11627.
28. Frisch M J, Trucks G W, Schlegel H B, Scuseria G E, Robb M A, Cheeseman J R, Scalmani G, Barone V, Mennucci B, Petersson G A, Nakatsuji H, Caricato M, Li X, Hratchian H P, Izmaylov A F, Bloino J, Zheng G, Sonnenberg J L, Hada M, Ehara M, Toyota K, Fukuda R, Hasegawa J, Ishida M, Nakajima T, Honda Y, Kitao O, Nakai H, Vreven T, Jr Montgomery J A, Peralta J E, Ogliaro F, Bearpark M, Heyd J J, Brothers E, Kudin K N, Staroverov V N, Kobayashi R, Normand J, Raghavachari K,

- Rendell A, Burant J C, Iyengar S S, Tomasi J, Cossi M, Rega N, Millam J M, Klene M, Knox J E, Cross J B, Bakken V, Adamo C, Jaramillo J, Gomperts R, Stratmann R E, Yazyev O, Austin A J, Cammi R, Pomelli C, Ochterski J W, Martin R L, Morokuma K, Zakrzewski V G, Voth G A, Salvador P, Dannenberg J J, Dapprich S, Daniels A D, Farkas O, Foresman J B, Ortiz J V, Cioslowski J and Fox D J, Gaussian 09, Revision-A.02-SMP, Gaussian, Inc., Wallingford CT, 2009.
29. ATK version 2008.10, QuantumWise A/S (www.quantumwise.com).
 30. Brandbyge M, Mozos J L, Ordejón P, Taylor J and Stokbro K, *Phys Rev B*, 2002, **65**(16), 165401-165417; DOI:10.1103/PhysRevB.65.165401
 31. Soler J M, Artacho E, Gale J D, García A, Junquera J, Ordejón P and Sánchez-Portal D, *J PhysCondens Matter.*, 2002, **14**, 2745-2779; DOI:10.1088/0953-8984/14/11/302
 32. Taylor J, Guo H and Wang J, *Phys Rev B*, 2001, **63**(24), 245408-245421; DOI:10.1103/PhysRevB.63.245408
 33. Perdew J P, Zunger A, *Phys Rev B*, 1981, **23**(10), 5048-5079; DOI:10.1103/PhysRevB.23.5048
 34. Datta S, *Electronic Transport in Mesoscopic Systems*, Cambridge University Press, New York, 1996
 35. Li Y W, Yao J H, Zou Z G, Yang J W and Le S R, *Comp Theor Chem.*, 2011, **976**(1-3), 135-140; DOI:10.1016/j.comptc.2011.08.014
 36. Li Y, Yao J, Liu C and Yang C, *J Mol Struct.*, 2008, **867**, 59-63; DOI:10.1016/j.theochem.2008.07.026
 37. Yao J, Li Y, Zou Z, Yang J and Yin Z, *Physica B*, 2011, **406**(20), 3969-3974; DOI:10.1016/j.physb.2011.07.040
 38. Gao N, Liu H, Yu C, Wanga N, Zhao J and Xie H, *Comp Theor Chem.*, 2011, **963**(1), 55-62; DOI:10.1016/j.comptc.2010.09.008
 39. Rocheleau P and Ernzerhof M, *J Chem Phys.*, 2009, **130**(18), 184704-184711; DOI:10.1063/1.3119299
 40. El-Hendawy M M, El-Nahas A M and Awad M K, *Org Electron.*, 2012, **13**(5), 807-814; DOI:10.1016/j.orgel.2012.01.010